Journal of Molecular Neuroscience (2018) 65:43–53
https://doi.org/10.1007/s12031-018-1067-5

microRNA-21 Confers Neuroprotection Against Cerebral Ischemia-Reperfusion Injury and Alleviates Blood-Brain Barrier Disruption in Rats via the MAPK Signaling Pathway

Xiaofeng Yao[1] · Yahui Wang[2] · Dongya Zhang[3]

Received: 7 March 2018 / Accepted: 11 April 2018 / Published online: 26 April 2018

Abstract

The mechanism contributing to blood-brain barrier (BBB) disruption, involved in poststroke edema and hemorrhagic transformation, is important but elusive. We investigated microRNA-21 (miR-21)-mediated mechanism in the disruption of BBB following cerebral ischemia-reperfusion (I/R) injury. Rats with cerebral I/R injury were prepared after middle cerebral artery occlusion and subsequent reperfusion. The underlying regulatory mechanisms of miR-382 were investigated with treatment of miR-382 mimics, miR-382 inhibitors, or SB203580 (an inhibitor of the MAPK signaling pathway) prior to I/R modeling. Compared with sham-operated rats, rats following I/R showed increased Longa's scores, ischemic hemisphere volume, cerebral infarct volume, EB content in brain tissues, enhanced levels of p38, iNOS, and MMP-9. The ectopic expression of miR-21 by mimics and MAPK signaling inhibition by SB203580 reduced Longa's scores, ischemic hemisphere volume, cerebral infarct volume, EB content in brain tissues, decreased levels of p38, MAP2K3, iNOS, and MMP-9. The luciferase activity determination showed miR-21 bound to MAP2K3 in its 3′UTR. miR-21 downregulation mediated by inhibitors appeared to yield an opposed trend. We also found that MAPK signaling inhibition by SB203580 could rescue rats with treatment of miR-382 inhibitors. The study highlights the neuroprotective role of MiR-21 during cerebral I/R injury and its preventive effect against BBB disruption by blocking the MAPK signaling pathway via targeted inhibition of MAP2K3, potentially opening a novel therapeutic avenue for the treatment of cerebral ischemia.

Keywords microRNA-21 · MAPK signaling pathway · Cerebral ischemia-reperfusion injury · Blood-brain barrier · Neuronal remodeling

Introduction

Cerebral ischemia is the loss or damage of neuronal function in the brain, which is commonly attributed to transient or permanent reduction in cerebral blood flow (Chumboatong et al. 2017; Hughes and Im 2016). Currently, reperfusion remains the standard therapy for ischemia to restore blood supply, but it usually generates reperfusion injury (Wu et al. 2017). Ischemia-reperfusion (I/R) injury has been manifested to be the third leading cause of death worldwide (Su et al. 2016). Cerebral I/R injury is followed by brain ischemia and exacerbated by an abrupt blood supply (Tang et al. 2016). Cerebral I/R injury cannot only aggravate cerebral injury and neurological impairment, but also enhance revascularization and cerebral infarction (Yu et al. 2015). The pathogeneses for tissue injuries following reperfusion include excessive production of reactive oxygen species, oxidative stress, mitochondrial dysfunction, and protein oxidation (Zhang et al. 2016). microRNAs (miRNAs) are also involved in the pathological processes of cerebral I/R injury, in spite of the poorly defined biological functions and signal transduction pathway (Min et al. 2015).

miRNAs are a class of highly conservative double-stranded non-coding RNAs with length of 19–24 nucleotides, which play crucial roles in mediating cell fate in neural stem cells in

✉ Dongya Zhang
zhangyadong7852@163.com

[1] Department of Neurosurgery, Xianyang Hospital, Yan'an University, Xianyang 712000, People's Republic of China

[2] Department of Gerontology, BaoJi Central Hospital, BaoJi 721008, People's Republic of China

[3] Department of Neurology, Xianyang hospital, Yan'an University, Wenlin Road, No. 38, Weicheng District, Xianyang 712000, People's Republic of China

the development of brain (Verma et al. 2016; Ma et al. 2017). miRNAs bind the target messenger RNAs (mRNAs) in the 3′ untranslated region (UTR) and silence the translation by RNA-induced silencing complexes (RISCs) on the basis of complementary base-pairing (Kadera et al. 2013). In the hippocampus, miRNAs are crucial effectors in neuronal development and regulators for sustainability of neuronal phenotype (Deng et al. 2013). Commonly, miRNAs, in the central nervous system, are associated with the occurrence and progression of multiple diseases, such as cerebral ischemic stroke (Sun et al. 2013), Parkinson's disease (Cho et al. 2013), and cerebral I/R/ injury (Tao et al. 2015; Liu et al. 2016), but how the miRNAs exert the effects remains to be determined. microRNA-21 (miR-21) is an anti-apoptotic factor in cell biological activities, and the effects of miR-21 have seldom been explored in neurologic diseases, especially cerebral I/R injury (Buller et al. 2010), though its roles have been pointed out in cell proliferation and apoptosis in spinal cord neurons (Jiao et al. 2015) and the malignant progression of glioma (Kwak et al. 2011). Mitogen-activated protein kinase (MAPK) is a class of serine/threonine kinases and transmits signals when activated by extracellular stimuli from cell membrane to the nucleus (Sun and Nan 2016; Hao et al. 2013). The MAPK signaling is implicated in production of inflammatory cytokines, neuronal death, and survival in brain injuries caused by ischemia and hemorrhage (Ansar et al. 2013). This present study aimed to identify the expression of miR-21 in rat models of cerebral I/R injury and its effects on neural function and BBB permeability through the MAPK signaling pathway.

Materials and Methods

Experimental Animals

Specific pathogen-free (SPF) male Sprague-Dawley (SD) rats ($n = 96$), weighing 220 ~ 240 g, were used for the following experiments. They were all purchased from Hunan Slac Laboratory Animals Co., Ltd. (Changsha, Hunan, China). Before being used in the experiments, the rats were allowed to adapt to the new conditions for 1 week, with free access to food and water. The environmental conditions were controlled of temperature (20 ~ 25 °C), relative humidity (60 ~ 70%). The rats were maintained without noise exposure for at least 24 h, and they were deprived of food but not water before surgery.

Establishment of Cerebral I/R Injury Rat Model

Before surgery, rats were deprived of food for 12 h, but allowed with free access to water. After weighing, rats were anesthetized by an intraperitoneal injection with 3% pentobarbital sodium (30 mg/kg body weight, Sigma Chemical Co., St. Louis, Missouri, USA). Being fixed on the operation table in the supine position, rats were shaved and disinfected conventionally. A midline incision of approximately 1.5 cm was made in the cervical region. Fascia superficialis was separated between submandibular glands of both sides. The sternocleidomastoid muscles and sternohyoid muscles were separated by blunt dissection, so as to expose the right common carotid artery (CCA) and fully separate internal carotid artery (ICA) and external carotid artery (ECA). The ECA and the CCA were also ligated at the distal and proximal ends. Then, the ICA was clamped with an artery clamp at the end proximal to the cranium. A thread was inserted below the CCA proximal to bifurcation and then ligated loosely. An opening was made between the left CCA ligation position and the bifurcation of CCA, and the thread occlusion was inserted into the opening. When the thread was tightened up, the artery clamp was loosened to restore blood supply. Along the ICA, the thread was sent to the cranium at a depth of 18 ~ 20 mm with slight resistance, which suggested that the tip of the thread reached the starting end of middle cerebral artery (MCA). In the sham group, the thread was ligated in the CCA, but it was not inserted into the MCA. Incisions were sutured layer by layer, and the end of the thread (approximately 1 cm) was left out of the skin incision. After the thread was inserted in the MCA for 90 min, the reserved thread was pulled out gently till resistance was felt. The starting end of the thread got back to the bifurcation of CCA. Then, blood supply of the MCA was recovered, and cerebral reperfusion was induced. After extra thread was cut off, rat models of cerebral I/R injury were established. General conditions of rats were observed until they recovered from anesthesia. On the basis of Zea Longa 5-point scale (Bushi et al. 2017), neurologic deficits were evaluated to verify establishment of cerebral I/R injury rat models.

Animal Grouping and Treatment

SD rats ($n = 96$) were classified into six groups. Sham group: the thread was ligated in the CCA without inserting into the MCA; I/R group: rat models of cerebral I/R injury, lateral ventricle was injected with dimethyl sulfoxide (DMSO, 5 μl) 30 min before ischemia (Kim et al. 2004; Chen et al. 1996); miR-21 mimic group: cerebral I/R injury + miR-21 mimic (synthesized by Guangzhou RiboBio Co., Ltd., Guangzhou, Guangdong, China), lateral ventricle was injected with miR-21 mimic (10 μl) 30 min before ischemia; miR-21 inhibitor group: cerebral I/R injury + miR-21 inhibitor (synthesized by Guangzhou RiboBio Co., Ltd., Guangzhou, Guangdong, China), lateral ventricle was injected with miR-21 inhibitor (10 μl) 30 min before ischemia; miR-21 inhibitor + SB203580 group: cerebral I/R injury + miR-21 inhibitor + SB203580 (inhibitor of the MAPK signaling pathway,

Sigma Chemical Co., St. Louis, Missouri, USA), lateral ventricle was injected with miR-21 inhibitor (10 μl) and SB203580 (5 μl, dissolved in 0.1 nmol/μl solution using 1% DMSO) 30 min before ischemia; SB203580 group: cerebral I/R injury + SB203580 (5 μl, dissolved in 0.1 nmol/μl solution using 1% DMSO) 30 min before ischemia. In each group, the solution was slowly injected (1 μl/min) after the syringe needle was inserted in the ventricle. After injection, the syringe needle was retained in the injection site for 3 min and then pulled out slowly. The injection sites on the surface of the cranium were sealed with bone wax, and the scalp was sutured and disinfected.

Zea Longa 5-Point Scale for Evaluation of Neurologic Deficits

Twenty-four hours following reperfusion, neurologic deficits in rats of all the six groups were assessed by Zea Longa 5-point scale (Bushi et al. 2017): 0, no deficit; 1, mild deficit, failure to extend left forepaw fully; 2, medium deficit, circling to the left lateral side; 3, falling to the contralateral side; and 4, severe deficit, no spontaneous walking, with a loss of consciousness.

Determination of Cerebral Edema Severity and Infarct Size

Rats (eight for each group) were intraperitoneally anesthetized with pentobarbital sodium and sacrificed by cervical dislocation 24 h after reperfusion. Intact brain tissues were extracted on the ice and stored immediately in a refrigerator for 30 min at − 20 °C. Then, brain tissues were sliced coronally to sections of 2 mm. Based on the method reported by Bederson et al. (1986), brain sections were incubated in 2% 2,3,5-triphenyltetrazolium chloride (TTC) solution in a warm water bath at 37 °C for 20 min. After staining, the sections were fixed in 4% paraformaldehyde for 24 h. According to the order of brain sections, the front and back sides were photographed, respectively, by a digital camera. ImageJ 1.42I software was performed to calculate the mean infarct size of the front and back sides, the mean ischemic hemisphere area of the front and back sides, the mean area of the other hemisphere of the front and back sides, edema severity, and the increased percentage of ischemic hemisphere volume of each brain section. On the basis of the method provided by Belayev et al. (1996), effect of cerebral edema on infarct size was corrected, and the percentage of infarct volume was calculated.

Determination of Blood-Brain Barrier Permeability

Eight rats were selected from each group. Twenty-four hours after reperfusion, rats were lightly anesthetized with pentobarbital sodium via intraperitoneal injection. Through the caudal vein, 2% Evans blue (EB) in normal saline (2 ml/kg) was injected. After injection of EB for 1 h, the anesthesia was deepened. The rats were fixed in the supine position. The thorax was opened immediately. A venous indwelling needle was intubated through the left ventricle to the aorta and fixed then. Along the indwelling needle, the heart was perfused and rinsed using normal saline with a pressure of 100 mmHg to wash EB in the vessels. The right atrial appendage was cut open. The perfusion was stopped when the effluent from the right atria turned clear, and each rat needed approximately 150 ml normal saline. After perfusion of normal saline in the heart, the rats were decapitated to extract the brain. The left and right cerebral hemispheres were separated, and the arachnoid membrane, blood clots, and choroid plexuses on the cortex were removed. Following that, the hemispheres were immersed in the formamide with known volume, and the volume of the brain was measured and recorded. Formamide was supplemented until it was five times of the volume of the brain. After water bath at 37 °C for 48 h, optical density (OD) values were determined at the wavelength of 620 nm, with formamide as the blank control. According to the standard curve, EB content (μg/ml) was measured, and the content of brain tissues (μg/ml) was five times of the content of EB.

Determination of Changes of Ultrastructure of BBB

The anesthetized rats were fixed on the operation table. The thorax was opened immediately. A venous indwelling needle was intubated through the left ventricle. The heart was perfused using normal saline. When the effluent from the right atria turned clear, the rats were perfuse-fixed with 2.5% glutaraldehyde fixing solution. The cranium was opened and brain tissues were extracted. Cortex of the right parietal lobe was extracted and cut into 1 mm^3 blocks with a double-edged blade. The cortex blocks were fixed in the above-mentioned fixing solution for 2 h, and then fixed in 1% osmic acid. After that, the blocks were dehydrated in graded ethanol, embedded in epoxy resin Epon 812, and sliced to ultrathin sections by an ultrathin slicer (Leica Microsystems GmbH, Wetzlar, Germany). After uranium and lead staining, sections were observed and photographed under a Hitachi 7500 transmission electron microscope.

Luciferase Reporter Gene Assay

The target gene analysis of miR-21 was performed using the biological prediction website microRNA.org and whether MAP2K3 was a target of miR-21 was verified using luciferase reporter gene assay. A complementary sequence mutation site of the seed sequence was designed based on the MAP2K3 wild type (WT). Plasmid extraction was conducted according to kit's instructions. The correct luciferase reporter plasmids of

WT and mutant type (MUT) were co-transfected into HEK-293T cells with miR-21 using Lipofectamine 2000 (Invitrogen, Carlsbad, California, USA) according to the manufacturer's instructions, respectively. Negative controls for MAP2K3-3′UTR-WT and MAP2K3-3′UTR-MUT were prepared. Cells were harvested at 48 h after transfection, in which the luciferase activity was allowed to be determined. At least three independent experiments were performed.

Reverse Transcription Quantitative Chain Reaction

Total RNA was extracted to determine the concentration and purity. According to the instructions of a reverse transcription kit (DRR047S, Takara Biotechnology Ltd., Dalian, Liaoning, China), the sample RNA was reversely transcribed into cDNA, with a total system of 10 μl. The reversely transcribed cDNA was diluted with 65 μl diethyl-pyrocarbonate (DEPC)-treated water, followed by full blending. The reaction system for RT-qPCR was set as follows: 5 μl of SsoFast EvaGreen Supermix (1708882, Bio-Rad, Hercules, CA, USA), 0.5 μl of forward primer (10 μM), and 0.5 μl reverse primer (10 μM) and 4 μl cDNA. The amplification conditions were 30 cycles of pre-denaturation at 95 °C for 1 min, denaturation at 95 °C for 30 s, and annealing at 58 °C for 5 s, followed by extension at 72 °C for 5 s. The primers were synthesized by Shanghai Invitrogen Biotech Co., Ltd. (Shanghai, China), and details are displayed in Table 1. Taking U6 and β-actin as the internal controls, each gene of each sample was repeated for three times. Melting curves were plotted to assess reliability of PCR results. The relative expression of target genes was calculated by the $2^{-\triangle\triangle Ct}$ method (Tuo et al. 2015) with the inflection point of amplification curve as Ct value: $\triangle Ct$ = Ct(target gene) − Ct(internal control), $\triangle\triangle Ct = \triangle Ct$ (experimental group) − $\triangle Ct$(control group). The experiment was repeated for three times.

Western Blotting

Protein levels of p38, iNOS, and MMP-9 in the brain tissues surrounding MCA and cerebral capillaries of rats were determined by Western blotting. The brain tissues were extracted and homogenized in lysis buffer, followed by standing for 30 min. After that, brain tissues were centrifugated (3000*g*) at 4 °C for 15 min, and the supernatant was collected and stored at − 20 °C for further use. Bovine serum albumin (BSA, 2 μg/μl) was diluted by phosphate-buffered saline (PBS) to concentrations of 20, 15, 10, 5, 2.5, and 0 μg/ml. A bicinchoninic acid (BCA) protein assay kit (Thermo Fisher Scientific, Inc., Waltham, MA, USA) was applied to measure protein concentration according to the instructions. Electrophoresis was performed at 4 °C with stacking gel at 80 V and running gel at 120 V. The separated proteins were transferred onto polyvinylidene fluoride (PVDF) membrane by wet transfer. Then, the proteins were blocked using 5% skim milk in Tris-buffered saline with Tween 20 (TBST), followed by incubation at room temperature for 2 h. The primary antibodies of p38 (1: 1000, Merck Millipore, Billerica, MA, USA), phosphorylated-p38 (p-p38, 1: 1000, Merck Millipore, Billerica, MA, USA), MAP2K3 (1 μg/ml, Abcam, Cambridge, UK), iNOS (1 μg/ml, Abcam PLC, Cambridge, UK), and MMP-9 (1 μg/ml, Abcam PLC, Cambridge, UK) were added to incubate at 4 °C overnight. After TBST washing for three times (10 min per wash), secondary antibodies (1:10,000, ProteinTech Group, Chicago, IL,

Table 1 Primer sequences for reverse transcription quantitative polymerase chain reaction

Gene	Primer sequence(5′-3′)
miR-21	Forward: 5′-ACACTCCAGCTGGGTAGCTTATCAGACTGAT-3′
	Reverse: 5′-ACTGGTGTCGTGGAGTCG-3′
U6	Forward: 5′-CCTGCTTCGGCAGCACA-3′
	Reverse: 5′-AACGCTTCACGAATTTGCGT-3′
p38MAPK	Forward: 5′-GTGATTGGTCTGTTGGATGTG-3′
	Reverse: 5′-TGGATTATGTCAGCCGAGTG-3′
MAP2K3	Forward: 5′-CGGCTGCAAGCCCTACAT-3′
	Reserse:5′-CTCCAGACGTCGGACTTGACA-3′
iNOS	Forward: 5′-GAAAGCGGTGTTCTTTGCTTCT-3′
	Reverse: 5′-CTTATACTGTTCCATGCAGACAACCT-3′
MMP-9	Forward: 5′-GTAACCCTGGTCACCGGACTT-3′
	Reverse: 5′-ATACGTTCCCGGCTGATCAG-3′
β-actin	Forward: 5′-GGCCCCTGCTGAAGCGTT-3′
	Reverse: 5′-GATTCCACGAGCCCCTTG--3′

miR-21 microRNA-21, *p38MAPK* p38 mitogen-activated protein kinase, *iNOS* inducible nitric oxide synthase, *MMP-9* matrix metalloproteinase 9

USA) were supplemented to incubate at room temperature for 1 h. Chemiluminescence was conducted, and the images of the gels were captured and analyzed.

Statistical Analysis

All the data were analyzed with SPSS 22.0 software (IBM Corp, Armonk, NY, USA). The quantitative data were presented as mean ± standard deviation. Comparisons among multiple groups were performed by one-way analysis of variance (ANOVA), and *t* test for comparisons between two groups when the data followed a normal distribution. The level of significance was $P < 0.05$.

Results

Up-Regulated miR-21 and Inhibited MAPK Signaling Pathway Attenuates Neurologic Deficits

Rats in the sham group did not show any neurological deficits. Longa's scores of the I/R group (2.51 ± 0.78) were significantly higher than that in the sham group ($P < 0.05$). The miR-21 mimic group (1.52 ± 0.65) and the SB203580 group (1.83 ± 0.70) exhibited lower Longa's scores than that in the I/R group ($P < 0.05$). The Longa's scores of the miR-21 inhibitor group (3.09 ± 0.81) were higher than the I/R group ($P < 0.05$). Compared with the SB203580 group, the Longa's scores of the miR-21 inhibitor + SB203580 group (2.74 ± 0.79) were increased ($P < 0.05$) (Fig. 1). miR-21 ameliorated neurologic deficits in rat models of cerebral I/R injury, and up-regulated miR-21 expression or suppressed MAPK signaling pathway repressed neurologic deficits.

Up-Regulated miR-21 and Inhibited MAPK Signaling Pathway Reduces Severity of Cerebral Edema

The ischemic hemisphere volume of rats in the sham group increased very little by 1.81 ± 1.42%. The I/R group showed an increased ischemic hemisphere volume of 21.48 ± 1.59%, which was larger than that in the sham group ($P < 0.05$). The ischemic hemisphere volumes of the miR-21 mimic and SB203580 groups increased, respectively, by 12.43 ± 1.63 and 16.23 ± 1.46%, which were significantly smaller than that in the I/R group ($P < 0.05$). The miR-21 inhibitor group had an increased ischemic hemisphere volume of 28.69 ± 1.87%, which was larger than the I/R group ($P < 0.05$). Compared with the SB203580 group, the miR-21 inhibitor + SB203580 group displayed an increased ischemic hemisphere volume of 23.25 ± 1.62% ($P < 0.05$) (Fig. 2). miR-21 decreased severity of cerebral edema in rat models of cerebral I/R injury. Inhibited miR-21 expression enhanced severity of cerebral edema, which was the opposite situation when the MAPK signaling pathway was inhibited.

Up-Regulated miR-21 and Inhibited MAPK Signaling Pathway Reduces Cerebral Infarct Size

Rats in the sham group did not show any infarct the ischemic hemisphere. The I/R group had an infarct volume of 28.56 ± 4.01%, which was significantly larger than that in the sham group ($P < 0.05$). The infarct volumes of the miR-21 mimic

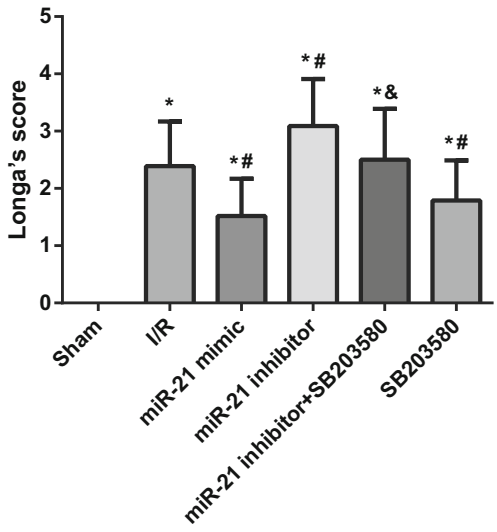

Fig. 1 Comparison on Longa's scores to assess neurological deficits in rats. Note: miR-21, microRNA-21; I/R, ischemia-reperfusion; *$P < 0.05$ compared with the sham group; #$P < 0.05$ compared with the I/R group; &$P < 0.05$ compared with the SB203580 group

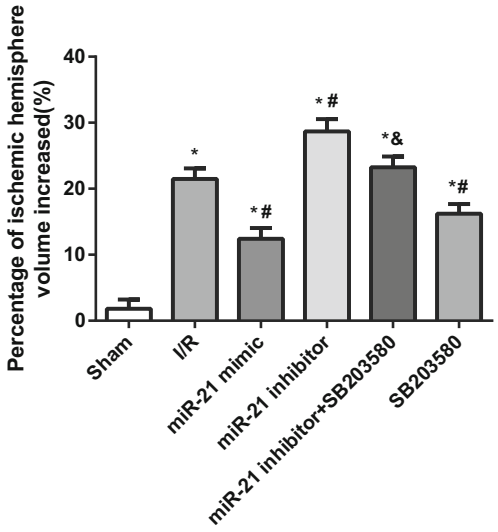

Fig. 2 Percentage of increased ischemic hemisphere volume in rats. Note: miR-21, microRNA-21; I/R, ischemia-reperfusion; *$P < 0.05$ compared with the sham group; #$P < 0.05$ compared with the I/R group; &$P < 0.05$ compared with the SB203580 group

and SB203580 groups were 20.15 ± 4.78 and 23.32 ± 2.76%, which were decreased when compared with the I/R group ($P < 0.05$). The miR-21 inhibitor group had an increased infarct volume of 35.24 ± 3.75%, as compared to the the I/R group ($P < 0.05$). In comparison to the SB203580 group, the miR-21 inhibitor + SB203580 group exhibited an elevated infarct volume of 29.39 ± 3.59% ($P < 0.05$) (Fig. 3). miR-21 decreased infarct volume in rat models with cerebral I/R injury. Suppressed miR-21 expression promoted increase of infarct size, while inhibition of the MAPK signaling pathway curtailed the progression of the cerebral infarct size caused by under-expressed miR-21.

Up-Regulated miR-21 and Inhibited MAPK Signaling Pathway Abates the Increase of BBB Permeability Disruption

The EB content in rat brain tissues of the sham group was 3.35 ± 1.26 μg/ml. The I/R group showed higher EB content of 52.34 ± 14.02 μg/ml than the sham group ($P < 0.05$). In comparison with the I/R group, the miR-21 mimic and SB203580 groups showed decreased EB contents of 27.75 ± 10.98 and 32.32 ± 11.32 μg/ml ($P < 0.05$). The miR-21 inhibitor group displayed an EB content of 76.02 ± 17.08 μg/ml, which was higher than the I/R group ($P < 0.05$). Compared with the SB203580 group, the miR-21 inhibitor + SB203580 group showed significantly increased EB content of 62.65 ± 17.28 μg/ml ($P < 0.05$) (Fig. 4). miR-21 decreased BBB permeability in rat models of cerebral I/R injury. Repressed miR-21 expression increased BBB permeability, but inhibitor of the MAPK signaling pathway reduced the increase of BBB permeability caused by miR-21 under-expression.

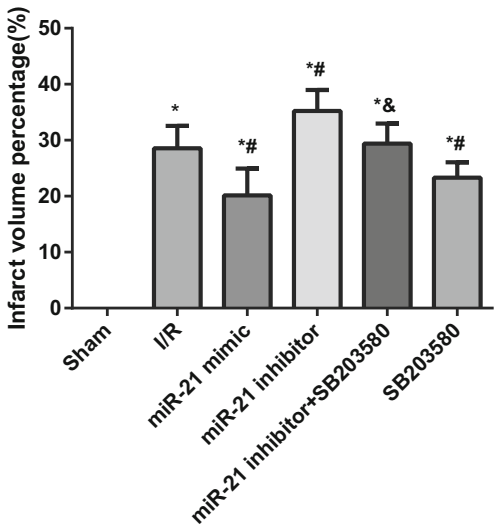

Fig. 3 Percentage of cerebral infarct volume in the ischemic hemisphere in rats. Note: miR-21, microRNA-21; I/R, ischemia-reperfusion; *$P < 0.05$ compared with the sham group; #$P < 0.05$ compared with the I/R group; &$P < 0.05$ compared with the SB203580 group

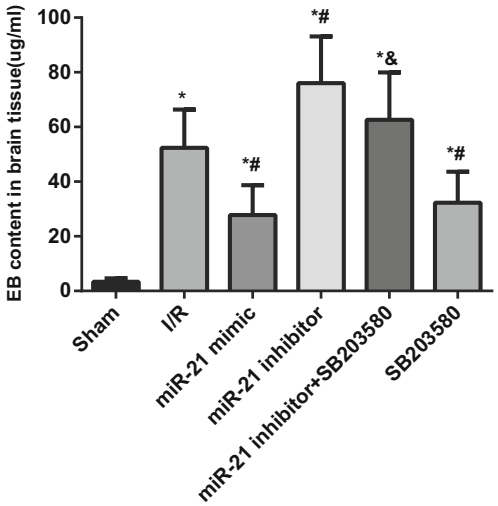

Fig. 4 Comparison on the EB content in rat brain tissues among six groups. Note: miR-21, microRNA-21; I/R, ischemia-reperfusion; EB, Evans blue; *$P < 0.05$ compared with the sham group; #$P < 0.05$ compared with the I/R group; &$P < 0.05$ compared with the SB203580 group

Changes of BBB Ultrastructure in Rats of Each Group

Rats in the sham group did not exhibit any obvious changes surrounding cerebral capillaries and in the lumen. Rats in the I/R group had severe edema surrounding capillaries in the cortex of ischemic reperfusion and squeezed lumen of capillaries. The miR-21 mimic and SB203580 groups showed mild edema surrounding capillaries and mild squeeze to lumen of capillaries. The miR-21 inhibitor group showed more severe edema and squeeze than the I/R group. The miR-21 inhibitor + SB203580 group had even more severe edema and squeeze than the SB203580 group (Fig. 5).

miR-21 Targets MAP2K3

Furthermore, we examined whether miR-21 could directly regulate MAP2K3 by means of target prediction program and luciferase activity determination. The results showed that MAP2K3 was the target gene of miR-21 (Fig. 6a), and there was a specific binding region between 3′UTR of the gene and the miR-382 sequence. The targeting relationship between miR-21 and MAP2K3 was verified by luciferase reporter gene assay (Fig. 6b). The results showed that the luciferase activity of MAP2K3 WT 3′-UTR was significantly inhibited by miR-21 ($p < 0.05$), while the luciferase activity of mutant 3′-UTR did not show the same effect ($p > 0.05$), indicating that miR-21 may specifically bind to MAP2K3-3′-UTR and downregulate MAP2K3 expression at post-transcriptional level. The results above indicated that miR-21 binds to MAP2K3 in its 3′UTR.

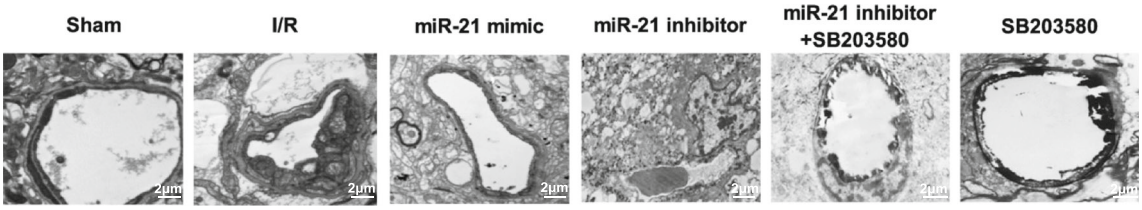

Fig. 5 The changes of blood-brain barrier ultrastructure in rats of six groups. Note: miR-21, microRNA-21; I/R, ischemia-reperfusion

Up-Regulated miR-21 Represses the Expression of MAPK Signaling Pathway-Related Genes

RT-qPCR (Fig. 7) was performed to measure miR-21 expression and mRNA levels of p38, MAP2K3, iNOS and MMP-9. The I/R group had lower miR-21 expression and higher mRNA levels of p38, MAP2K3, iNOS, and MMP-9 than those in the sham group ($P < 0.05$). Compared with the I/R group, the miR-21 mimic and SB203580 groups showed increased miR-21 expression and reduced mRNA levels of p38, MAP2K3, iNOS, and MMP-9 ($P < 0.05$), while the miR-21 inhibitor group displayed an opposite tendency ($P < 0.05$). In comparison with the SB203580 group, the miR-21 expression was decreased and the mRNA levels of p38, MAP2K3, iNOS, and MMP-9 were elevated in the miR-21 inhibitor + SB203580 group ($P < 0.05$).

Up-Regulated miR-21 Represses the Expression of MAPK Signaling Pathway-Related Proteins

Protein expressions of p38, MAP2K3, iNOS, and MMP-9 were determined by Western blotting (Fig. 8). The I/R group showed higher protein expression of p-p38/p38, MAP2K3, iNOS, and MMP-9 than the sham group ($P < 0.05$). Compared with the I/R group, the miR-21 mimic and SB203580 groups had decreased protein expression of p-p38/p38, MAP2K3, iNOS, and MMP-9, while those in the the miR-21 inhibitor group was increased ($P < 0.05$). In comparison to the SB203580 group, the miR-21 inhibitor + SB203580 group displayed higher protein expression of p-p38/p38, MAP2K3, iNOS, and MMP-9 ($P < 0.05$).

Discussion

Cerebral I/R injury is a serious challenge for the post-ischemia treatment, since its injuries on the brain tissues are permanent (Zhang et al. 2016). miR-21 has been proven to serve as critical regulators in the central nervous system (Zhang et al. 2012) and function recovery caused by I/R reperfusion injury (Hu et al. 2014; Yang et al. 2015). This present study explored how miR-21 influences neural function and BBB permeability in rat models of cerebral I/R injury through the MAPK signaling pathway, in an attempt to find a novel therapeutic target.

Based on the results of RT-qPCR, miR-21 levels were reduced in rats with cerebral I/R injury. When neural functions and BBB permeability were detected, we found that up-regulated miR-21 curtailed the neurologic deficits, severity

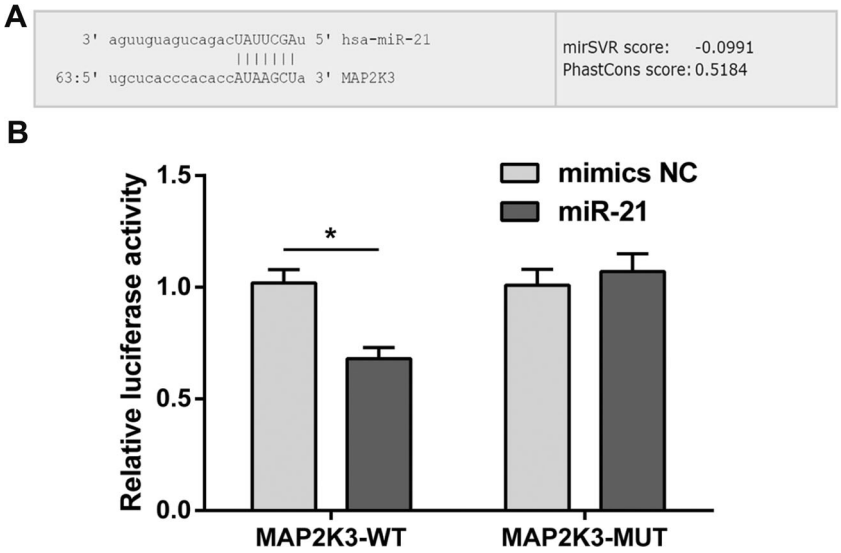

Fig. 6 MAP2K3 is a target gene of miR-21 by the target prediction program and determination of luciferase activity. **a** miR-21 binds to the 3′UTR of MAP2K3. **b** The luciferase activity is decreased after treatment by a combination of miR-21 mimics and MAP2K3-3′UTR-wt; *$P < 0.05$ compared with the mimic NC

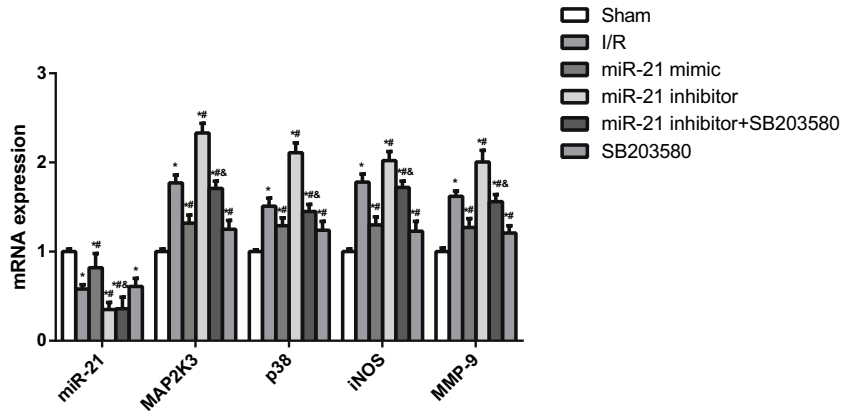

Fig. 7 Comparison on miR-21 expression and mRNA expression of p38, iNOS, and MMP-9 in rat brain tissues of six groups detected by RT-qPCR. Note: miR-21, microRNA-21; I/R, ischemia-reperfusion; iNOS, inducible nitric oxide synthase; MMP-9, matrix metalloproteinase 9; RT-qPCR, reverse transcription quantitative polymerase chain reaction; $*P < 0.05$ compared with the sham group; $\#P < 0.05$ compared with the I/R group; $\&P < 0.05$ compared with the SB203580 group

of edema, infarct volume, BBB permeability disruption, and exacerbation of BBB ultrastructure changes. When exposed to ischemic conditions and reperfusion, neurons and astrocytes showed altered miR-21 expression levels (Min et al. 2015). Moreover, miR-21 has also been demonstrated to be lowly expressed in myocardial ischemia injury, and it suppresses cardiocyte apoptosis induced by hypoxia-reperfusion (Yang et al. 2014). miR-21 has been verified to be an anti-apoptotic and protective factor in cerebral ischemia by reducing the expression levels of Fas ligand (FASLG) (Zhou and Zhang 2014). Specifically, miR-21 is of significance in decreasing ischemic cell death through targeting the ligand inducing cell death, and its overexpression confers neuroprotection against neuronal death caused by ischemia (Buller et al. 2010). In cardiac I/R injury, when miR-21 levels are raised, its protective effects are strengthened through regulating Akt and the Bcl-2/Bax signaling pathway (Ma et al. 2016). On the other hand, In diabetes mellitus combined with cerebral infarction, miR-21 improves nerve defects by enhancing nerve regeneration and suppressing apoptosis of neurons through inhibition of programmed cell death protein 4 (Guo et al. 2017). Similar to our findings, upregulation of miR-21 decreases the infarct volume in models of I/R injury, as well as enhances ventricular remodeling (Qin et al. 2012; Qiao et al. 2015). The study of Ge et al. provides consistent results with our study, which highlights that upregulation of miR-21 expression attenuates neurological impairment after traumatic brain injury, as well as ameliorates brain edema which is associated with BBB leakage in rats (Ge et al. 2015). Inhibition of miR-21 expression represses the expression of the downstream target MMP-9, which is involved in the pathogenesis of BBB permeability increase and formation of infarct after cerebral ischemia (Di et al. 2014). In the study of Friedman (Buatti et al. 1996), they raised cats under irradiation. The Evans blue was detected in cats due to long-time irradiations leading to stress, even the cat brains were protected by U74389G. But in our study, the animal treatment was performed according to the international guidance for animal care and use, and animals were anesthetic prior to I/R modeling and the Evans blue staining. Psychological stress occurring may be the reason for low

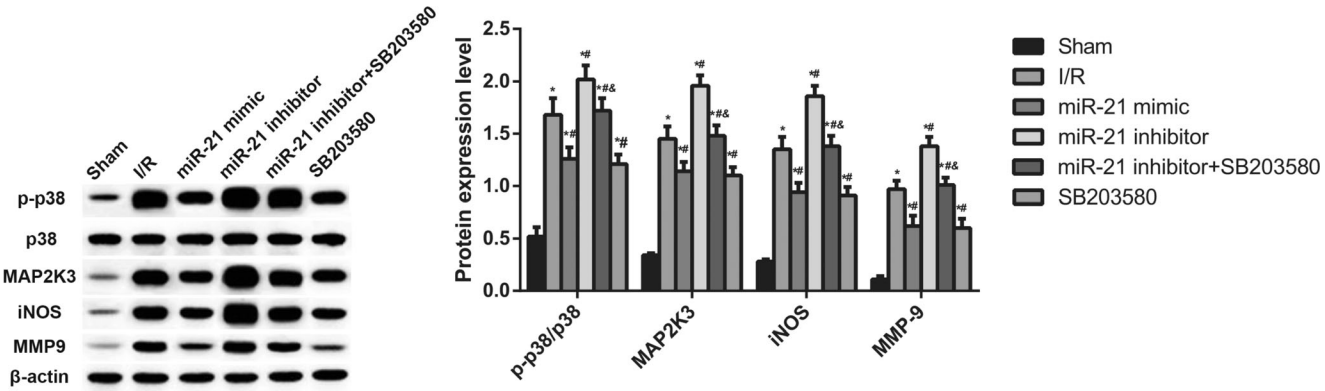

Fig. 8 Comparison on protein expression of p-p38/p38, iNOS, and MMP-9 in rat brain tissues of six groups detected by Western blotting. Note: miR-21, microRNA-21; I/R, ischemia-reperfusion; p-p38, phosphorylated-p38; iNOS, inducible nitric oxide synthase; MMP-9, matrix metalloproteinase 9; $*P < 0.05$ compared with the sham group; $\#P < 0.05$ compared with the I/R group; $\&P < 0.05$ compared with the SB203580 group

content of Evans blue determined in sham-operated rats. The extent is so minimal that we can neglect it.

In order to identify the activity of the MAPK signaling pathway in cerebral I/R injury and its relationship with miR-21, we initially performed luciferase reporter gene assay and found that targeted inhibition of MAP2K3 is responsible for the impact of miR-21 on the p38/MAPK signaling pathway. We also performed RT-qPCR and Western blotting and determined the increased mRNA and protein levels of p38, iNOS, and MMP-9 in cerebral I/R injury, which were decreased when miR-21 expression was boosted. Previous studies have documented that miR-21 regulated cell activity through the ERK/MAPK signaling pathway (Mei et al. 2013; Liu et al. 2013). miR-21a-5p is reported to bind to MAP2K3 which is an upstream activator of p38/MAPK signaling pathway in metabolic diseases (Xie et al. 2016). Activation of p38/MAPK can be driven by either of the immediate upstream kinases, MAP kinase (MAP2K)3 or MAP2K6, and recent evidence suggests that MAP2K3 has non-redundant roles in the pathology attributed to p38/MAPK activation (Lim et al. 2009). Corroborating findings are identified in previous studies, which indicate that activation of p38 is determined in neurons, microglia, and astrocyte, while inhibition of p38 expression is protective against ischemic stroke in reducing brain injury and inflammation (Roy Choudhury et al. 2014; Kovalska et al. 2012). In terms of iNOS, a remarkably increased expression and its relationship with cerebral I/R have been reported in Allen et al. study, which also reveals that down-regulated iNOS reduces cerebral infarct sizes (Heeba and El-Hanafy 2012). The underlying mechanism may be that oxidative stress plays a key role in the pathogenesis of cerebral I/R and exacerbates the brain injury (Allen and Bayraktutan 2009). Consistent findings have been demonstrated in the study of Deng et al., which suggests that MMP-9 promotes the degradation of basement membrane surrounding the cerebral capillaries and the increase of BBB permeability, and further accelerates the revascularization following ischemic injury (Deng et al. 2013). Furthermore, activated MAPK signaling disrupts BBB permeability and exacerbates ischemic injury by facilitating expression of inflammatory cytokines and adhesion molecules in the endothelial cells (Sun and Nan 2016). Previous studies also manifested that cerebral I/R injury was alleviated with reduced neurological deficits and infarct volume, oxidative stress, and cell apoptosis, when the activation of the MAPK signaling pathway was inhibited by UCF-101 or Fucoidan (Su et al. 2016; Che et al. 2017).

Taken together, the findings described above indicated that up-regulated miR-21 expression protected against cerebral I/R injury by restoring neural functions and abating BBB permeability disruption through inhibiting the activation of the MAPK signaling pathway. miR-21 may serve to understand the underlying molecular mechanisms in the function change and structural integrity of neuronal cells following cerebral I/R injury. In spite of the limited sample size, this study provides a potential miR-21-based target in treating cerebral I/R injury.

Acknowledgments The authors thank the reviewers for their helpful comments.

Compliance with Ethical Standards

The experimental protocols of the present study were approved by the Animal Care Committee at Xianyang hospital, Yan'an University.

Conflict of Interest The authors declare that they have no conflicts of interest.

References

Allen CL, Bayraktutan U (2009) Oxidative stress and its role in the pathogenesis of ischaemic stroke. Int J Stroke : Official J Int Stroke Soc 4(6):461–470. https://doi.org/10.1111/j.1747-4949.2009.00387.x

Ansar S, Eftekhari S, Waldsee R, Nilsson E, Nilsson O, Saveland H, Edvinsson L (2013) MAPK signaling pathway regulates cerebrovascular receptor expression in human cerebral arteries. BMC Neurosci 14:12. https://doi.org/10.1186/1471-2202-14-12

Belayev L, Busto R, Zhao W, Ginsberg MD (1996) Quantitative evaluation of blood-brain barrier permeability following middle cerebral artery occlusion in rats. Brain Res 739(1–2):88–96

Bederson JB, Pitts LH, Germano SM, Nishimura MC, Davis RL, Bartkowski HM (1986) Evaluation of 2,3,5-triphenyltetrazolium chloride as a stain for detection and quantification of experimental cerebral infarction in rats. Stroke 17(6):1304–1308

Buatti JM, Friedman WA, Theele DP, Bova FJ, Mendenhall WM (1996) The lazaroid U74389G protects normal brain from stereotactic radiosurgery-induced radiation injury. Int J Radiat Oncol Biol Phys 34(3):591–597

Buller B, Liu X, Wang X, Zhang RL, Zhang L, Hozeska-Solgot A, Chopp M, Zhang ZG (2010) MicroRNA-21 protects neurons from ischemic death. FEBS J 277(20):4299–4307. https://doi.org/10.1111/j.1742-4658.2010.07818.x

Bushi D, Stein ES, Golderman V, Feingold E, Gera O, Chapman J, Tanne D (2017) A linear temporal increase in thrombin activity and loss of its receptor in mouse brain following ischemic stroke. Front Neurol 8:138. https://doi.org/10.3389/fneur.2017.00138

Che N, Ma Y, Xin Y (2017) Protective role of Fucoidan in cerebral ischemia-reperfusion injury through inhibition of MAPK signaling pathway. Biomol Ther 25(3):272–278. https://doi.org/10.4062/biomolther.2016.098

Chen J, Graham SH, Zhu RL, Simon RP (1996) Stress proteins and tolerance to focal cerebral ischemia. J Cerebral Blood Flow Metabolism : Official J Int Soc Cerebral Blood Flow Metabolism 16(4):566–577. https://doi.org/10.1097/00004647-199607000-00006

Cho HJ, Liu G, Jin SM, Parisiadou L, Xie C, Yu J, Sun L, Ma B, Ding J, Vancraenenbroeck R, Lobbestael E, Baekelandt V, Taymans JM, He P, Troncoso JC, Shen Y, Cai H (2013) MicroRNA-205 regulates the expression of Parkinson's disease-related leucine-rich repeat kinase 2 protein. Hum Mol Genet 22(3):608–620. https://doi.org/10.1093/hmg/dds470

Chumboatong W, Thummayot S, Govitrapong P, Tocharus C, Jittiwat J, Tocharus J (2017) Neuroprotection of agomelatine against cerebral ischemia/reperfusion injury through an antiapoptotic pathway in rat.

Neurochem Int 102:114–122. https://doi.org/10.1016/j.neuint.2016.12.011

Deng X, Zhong Y, Gu L, Shen W, Guo J (2013) MiR-21 involve in ERK-mediated upregulation of MMP9 in the rat hippocampus following cerebral ischemia. Brain Res Bull 94:56–62. https://doi.org/10.1016/j.brainresbull.2013.02.007

Di Y, Lei Y, Yu F, Changfeng F, Song W, Xuming M (2014) MicroRNAs expression and function in cerebral ischemia reperfusion injury. J Molecular Neuroscience: MN 53(2):242–250. https://doi.org/10.1007/s12031-014-0293-8

Ge X, Han Z, Chen F, Wang H, Zhang B, Jiang R, Lei P, Zhang J (2015) MiR-21 alleviates secondary blood-brain barrier damage after traumatic brain injury in rats. Brain Res 1603:150–157. https://doi.org/10.1016/j.brainres.2015.01.009

Guo YB, Ji TF, Zhou HW, Yu JL (2017) Effects of microRNA-21 on nerve cell regeneration and neural function recovery in diabetes mellitus combined with cerebral infarction rats by targeting PDCD4. Mol Neurobiol 55:2494–2505. https://doi.org/10.1007/s12035-017-0484-8

Hao JL, Li YF, Li RS (2013) A novel mechanism of NALP3 inducing ischemia reperfusion injury by activating MAPK pathway in acute renal failure. Med Hypotheses 80(4):463–465. https://doi.org/10.1016/j.mehy.2012.12.041

Heeba GH, El-Hanafy AA (2012) Nebivolol regulates eNOS and iNOS expressions and alleviates oxidative stress in cerebral ischemia/reperfusion injury in rats. Life Sci 90(11–12):388–395. https://doi.org/10.1016/j.lfs.2011.12.001

Hu H, Jiang W, Xi X, Zou C, Ye Z (2014) MicroRNA-21 attenuates renal ischemia reperfusion injury via targeting caspase signaling in mice. Am J Nephrol 40(3):215–223. https://doi.org/10.1159/000368202

Hughes JN, Im MH (2016) Teacher-student relationship and peer disliking and liking across grades 1-4. Child Dev 87(2):593–611. https://doi.org/10.1111/cdev.12477

Jiao G, Pan B, Zhou Z, Zhou L, Li Z, Zhang Z (2015) MicroRNA-21 regulates cell proliferation and apoptosis in H(2)O(2)-stimulated rat spinal cord neurons. Mol Med Rep 12(5):7011–7016. https://doi.org/10.3892/mmr.2015.4265

Kadera BE, Li L, Toste PA, Wu N, Adams C, Dawson DW, Donahue TR (2013) MicroRNA-21 in pancreatic ductal adenocarcinoma tumor-associated fibroblasts promotes metastasis. PLoS One 8(8):e71978. https://doi.org/10.1371/journal.pone.0071978

Kim SW, Yu YM, Piao CS, Kim JB, Lee JK (2004) Inhibition of delayed induction of p38 mitogen-activated protein kinase attenuates kainic acid-induced neuronal loss in the hippocampus. Brain Res 1007(1–2):188–191. https://doi.org/10.1016/j.brainres.2004.02.009

Kovalska M, Kovalska L, Pavlikova M, Janickova M, Mikuskova K, Adamkov M, Kaplan P, Tatarkova Z, Lehotsky J (2012) Intracellular signaling MAPK pathway after cerebral ischemia-reperfusion injury. Neurochem Res 37(7):1568–1577. https://doi.org/10.1007/s11064-012-0752-y

Kwak HJ, Kim YJ, Chun KR, Woo YM, Park SJ, Jeong JA, Jo SH, Kim TH, Min HS, Chae JS, Choi EJ, Kim G, Shin SH, Gwak HS, Kim SK, Hong EK, Lee GK, Choi KH, Kim JH, Yoo H, Park JB, Lee SH (2011) Downregulation of Spry2 by miR-21 triggers malignancy in human gliomas. Oncogene 30(21):2433–2442. https://doi.org/10.1038/onc.2010.620

Lim AK, Nikolic-Paterson DJ, Ma FY, Ozols E, Thomas MC, Flavell RA, Davis RJ, Tesch GH (2009) Role of MKK3-p38 MAPK signalling in the development of type 2 diabetes and renal injury in obese db/db mice. Diabetologia 52(2):347–358. https://doi.org/10.1007/s00125-008-1215-5

Liu F, Zheng S, Liu T, Liu Q, Liang M, Li X, Sheyhidin I, Lu X, Liu W (2013) MicroRNA-21 promotes the proliferation and inhibits apoptosis in Eca109 via activating ERK1/2/MAPK pathway. Mol Cell Biochem 381(1–2):115–125. https://doi.org/10.1007/s11010-013-1693-8

Liu X, Li Z, Song Y, Wang R, Han L, Wang Q, Jiang K, Kang C, Zhang Q (2016) AURKA induces EMT by regulating histone modification through Wnt/beta-catenin and PI3K/Akt signaling pathway in gastric cancer. Oncotarget 7(22):33152–33164. https://doi.org/10.18632/oncotarget.8888

Min XL, Wang TY, Cao Y, Liu J, Li JT, Wang TH (2015) MicroRNAs: a novel promising therapeutic target for cerebral ischemia/reperfusion injury? Neural Regen Res 10(11):1799–1808. https://doi.org/10.4103/1673-5374.170302

Ma N, Bai J, Zhang W, Luo H, Zhang X, Liu D, Qiao C (2016) Trimetazidine protects against cardiac ischemia/reperfusion injury via effects on cardiac miRNA21 expression, Akt and the Bcl2/Bax pathway. Mol Med Rep 14(5):4216–4222. https://doi.org/10.3892/mmr.2016.5773

Ma J, Shui S, Han X, Guo D, Li T, Yan L (2017) microRNA-200a silencing protects neural stem cells against cerebral ischemia/reperfusion injury. PLoS One 12(2):e0172178. https://doi.org/10.1371/journal.pone.0172178

Mei Y, Bian C, Li J, Du Z, Zhou H, Yang Z, Zhao RC (2013) miR-21 modulates the ERK-MAPK signaling pathway by regulating SPRY2 expression during human mesenchymal stem cell differentiation. J Cell Biochem 114(6):1374–1384. https://doi.org/10.1002/jcb.24479

Qin Y, Yu Y, Dong H, Bian X, Guo X, Dong S (2012) MicroRNA 21 inhibits left ventricular remodeling in the early phase of rat model with ischemia-reperfusion injury by suppressing cell apoptosis. Int J Med Sci 9(6):413–423. https://doi.org/10.7150/ijms.4514

Qiao S, Olson JM, Paterson M, Yan Y, Zaja I, Liu Y, Riess ML, Kersten JR, Liang M, Warltier DC, Bosnjak ZJ, Ge ZD (2015) MicroRNA-21 mediates Isoflurane-induced Cardioprotection against ischemia-reperfusion injury via Akt/nitric oxide synthase/mitochondrial permeability transition pore pathway. Anesthesiology 123(4):786–798. https://doi.org/10.1097/ALN.0000000000000807

Roy Choudhury G, Ryou MG, Poteet E, Wen Y, He R, Sun F, Yuan F, Jin K, Yang SH (2014) Involvement of p38 MAPK in reactive astrogliosis induced by ischemic stroke. Brain Res 1551:45–58. https://doi.org/10.1016/j.brainres.2014.01.013

Su D, Ma J, Zhang Z, Tian Y, Shen B (2016) Protective effects of UCF-101 on cerebral ischemia-reperfusion (CIR) is depended on the MAPK/p38/ERK signaling pathway. Cell Mol Neurobiol 36(6):907–914. https://doi.org/10.1007/s10571-015-0275-6

Sun J, Nan G (2016) The mitogen-activated protein kinase (MAPK) signaling pathway as a discovery target in stroke. J Molecular Neuroscience: MN 59(1):90–98. https://doi.org/10.1007/s12031-016-0717-8

Sun Y, Gui H, Li Q, Luo ZM, Zheng MJ, Duan JL, Liu X (2013) MicroRNA-124 protects neurons against apoptosis in cerebral ischemic stroke. CNS Neuroscience Therapeutics 19(10):813–819. https://doi.org/10.1111/cns.12142

Tang XJ, Yang MH, Cao G, Lu JT, Luo J, Dai LJ, Huang KM, Zhang LI (2016) Protective effect of microRNA-138 against cerebral ischemia/reperfusion injury in rats. Experimental Therapeutic Medicine 11(3):1045–1050. https://doi.org/10.3892/etm.2016.3021

Tao Z, Zhao H, Wang R, Liu P, Yan F, Zhang C, Ji X, Luo Y (2015) Neuroprotective effect of microRNA-99a against focal cerebral ischemia-reperfusion injury in mice. J Neurol Sci 355(1–2):113–119. https://doi.org/10.1016/j.jns.2015.05.036

Tuo YL, Li XM, Luo J (2015) Long noncoding RNA UCA1 modulates breast cancer cell growth and apoptosis through decreasing tumor suppressive miR-143. European Rev Medical Pharmacological Sci 19(18):3403–3411

Verma P, Pandey RK, Prajapati P, Prajapati VK (2016) Circulating MicroRNAs: potential and emerging biomarkers for diagnosis of human infectious diseases. Front Microbiol 7:1274. https://doi.org/10.3389/fmicb.2016.01274

Wu G, Zhu L, Yuan X, Chen H, Xiong R, Zhang S, Cheng H, Shen Y, An H, Li T, Li H, Zhang W (2017) Britanin ameliorates cerebral ischemia-reperfusion injury by inducing the Nrf2 protective pathway. Antioxid Redox Signal 27:754–768. https://doi.org/10.1089/ars.2016.6885

Xie X, Song J, Li G (2016) MiR-21a-5p suppresses bisphenol A-induced pre-adipocyte differentiation by targeting map2k3 through MKK3/p38/MAPK. Biochem Biophys Res Commun 473(1):140–146. https://doi.org/10.1016/j.bbrc.2016.03.066

Yang Q, Yang K, Li A (2014) microRNA-21 protects against ischemia-reperfusion and hypoxia-reperfusion-induced cardiocyte apoptosis via the phosphatase and tensin homolog/Akt-dependent mechanism. Mol Med Rep 9(6):2213–2220. https://doi.org/10.3892/mmr.2014.2068

Yang W, Shao J, Bai X, Zhang G (2015) Expression of plasma microRNA-1/21/ 208a/499 in myocardial ischemic reperfusion injury. Cardiology 130(4):237–241. https://doi.org/10.1159/000371792

Yu H, Wu M, Zhao P, Huang Y, Wang W, Yin W (2015) Neuroprotective effects of viral overexpression of microRNA-22 in rat and cell models of cerebral ischemia-reperfusion injury. J Cell Biochem 116(2):233–241. https://doi.org/10.1002/jcb.24960

Zhang L, Dong LY, Li YJ, Hong Z, Wei WS (2012) miR-21 represses FasL in microglia and protects against microglia-mediated neuronal cell death following hypoxia/ischemia. Glia 60(12):1888–1895. https://doi.org/10.1002/glia.22404

Zhang JF, Shi LL, Zhang L, Zhao ZH, Liang F, Xu X, Zhao LY, Yang PB, Zhang JS, Tian YF (2016) MicroRNA-25 negatively regulates cerebral ischemia/reperfusion injury-induced cell apoptosis through Fas/FasL pathway. J Molecular Neuroscience : MN 58(4):507–516. https://doi.org/10.1007/s12031-016-0712-0

Zhou J, Zhang J (2014) Identification of miRNA-21 and miRNA-24 in plasma as potential early stage markers of acute cerebral infarction. Mol Med Rep 10(2):971–976. https://doi.org/10.3892/mmr.2014.2245